



Arterial, Venous, and Cerebrospinal Fluid Flow and Pulsatility in Stroke-Related Cerebral Small Vessel Disease: A Longitudinal Analysis

Alasdair G. Morgan, PhD; Michael J. Thrippleton¹, PhD; Michael S. Stringer¹, PhD; Francesca M. Chappell¹, PhD; Maria C. Valdés-Hernández¹, PhD; Stewart Wiseman¹, PhD; Lucia Ballerini¹, PhD; Rosalind Brown¹, PhD; Yajun Cheng¹, PhD; Xiaodi Liu¹, PhD; Junfang Zhang¹, PhD; Eleni Sakka¹, MSc; Daniela Jamie Garcia¹, PhD; Emilie Sleight¹, PhD; Cameron Manning, PhD; Roberto D. Coello¹, PhD; Dominic Job¹, PhD; Angela Jochems¹, PhD; Carmen Arteaga Reyes¹, MD; Una Clancy¹, PhD; Ian Marshall, PhD; Fergus N. Doubal¹, PhD; Joanna M. Wardlaw¹, MD

BACKGROUND: Cerebral small vessel disease (SVD) causes up to 45% of dementias and 25% of ischemic strokes, but the understanding of vascular pathophysiology is limited. We aimed to investigate the contribution of pulsatility of intracranial arteries, veins, and cerebrospinal fluid (CSF) and cerebral blood flow to long-term imaging and clinical outcomes in SVD.

METHODS: We prospectively recruited participants in Edinburgh/Lothian, Scotland, with lacunar or nonlacunar ischemic stroke (modified Rankin Scale score ≤ 2 , as controls) and assessed medical and brain magnetic resonance imaging characteristics at baseline and 1 year (2018–2022). We used phase-contrast magnetic resonance imaging to measure flow and pulsatility in major cerebral vessels and CSF to investigate independent associations with baseline white matter hyperintensity (WMH) and perivascular space (PVS) volumes and their progression, as well as with recurrent stroke, functional, and cognitive outcomes at 1 year. We applied linear, logistic, and ordinal regression models in our analysis.

RESULTS: We recruited 210 participants; 205 (66.8% male; aged 66.4 ± 11.1 years) had useable data. In covariate-adjusted analyses, higher baseline arterial pulsatility was associated with larger volumes of baseline WMH ($B=0.26$ [95% CI, 0.08–0.44]; $P=0.01$) and basal ganglia PVS ($B=0.12$ [95% CI, 0.04–0.20]; $P<0.01$) but not with their change at 1 year (WMH: $B=0.01$ [95% CI, -0.05 to 0.06]; $P=0.78$; basal ganglia PVS: $B=0.02$ [95% CI, -0.04 to -0.07]; $P=0.62$) or cognition, dependency, or recurrent stroke at 1 year. Neither cerebral blood flow nor CSF pulsatility was related to baseline SVD severity, WMH/PVS progression, or clinical outcomes at 1 year.

CONCLUSIONS: Associations between vascular/CSF pulsatility, cerebral blood flow, WMH/PVS, and clinical SVD features are complex. The lack of association between intracranial arterial, venous, or CSF pulsatility, cerebral blood flow, and WMH or PVS longitudinal change in this large, covariate-adjusted analysis questions the presumption that high intracranial vascular pulsatility causes SVD and its progression, consistent with other recent longitudinal studies. Intracranial pulsatility may differ from systemic vascular measures in their cause-pathogenic role(s) in SVD and should be considered separately.

GRAPHIC ABSTRACT: A [graphic abstract](#) is available for this article.

Key Words: carotid artery, internal ■ cerebral arteries ■ cerebral small vessel diseases ■ cranial sinuses ■ extracellular fluid ■ stroke, lacunar ■ vascular stiffness

Correspondence to: Joanna M. Wardlaw, MD, Department of Neuroimaging Sciences, Centre for Clinical Brain Sciences, The University of Edinburgh, 49 Little France Crescent, Edinburgh EH16 4SB, United Kingdom. Email joanna.wardlaw@ed.ac.uk

Supplemental Material is available at <https://www.ahajournals.org/doi/suppl/10.1161/STROKEAHA.124.049103>.

For Sources of Funding and Disclosures, see page 2461.

© 2025 The Authors. *Stroke* is published on behalf of the American Heart Association, Inc., by Wolters Kluwer Health, Inc. This is an open access article under the terms of the [Creative Commons Attribution](#) License, which permits use, distribution, and reproduction in any medium, provided that the original work is properly cited.

Stroke is available at www.ahajournals.org/journal/str

Nonstandard Abbreviations and Acronyms

BG	basal ganglia
BP	blood pressure
CBF	cerebral blood flow
CSF	cerebrospinal fluid
CSO	centrum semiovale
FVP	flow volume pulsatility
ICA	internal carotid artery
ICV	intracranial volume
MRI	magnetic resonance imaging
mRS	modified Rankin Scale
MSS3	Mild Stroke Study 3
OR	odds ratio
PC	phase contrast
PI	pulsatility index
PTT	pulse transit time
PVS	perivascular space
PWV	pulse wave velocity
ROI	region of interest
SVD	small vessel disease
WMH	white matter hyperintensity

Arterial stiffening is associated with several vascular pathologies, including stroke¹ and cerebral small vessel disease (SVD).² Arterial stiffness is increased by elastin loss, collagen replacement, and other factors,³ reducing vessel compliance.⁴ The resulting higher pulsatile stress can be measured in vivo using phase-contrast magnetic resonance imaging (PC-MRI) in larger blood vessels and may be transmitted to downstream blood vessels, causing tissue damage.⁵

Increased intracranial vessel pulsatility is associated with SVD.^{5–8} However, some studies show that neither cerebral blood flow (CBF)⁹ nor middle cerebral artery,¹⁰ internal carotid arteries (ICAs),¹¹ or small distal cerebral artery pulsatility¹¹ predicts white matter hyperintensity (WMH) progression. An increase in systemic large artery stiffness, measured via carotid-femoral pulse wave velocity (PWV), was the only vascular factor that occurred before the progression of small vessel disease (SVD) or cognitive decline.¹²

Cerebrospinal fluid (CSF) dynamics are integral to intracranial fluid physiology and can be assessed contemporaneously by PC-MRI, providing more information about brain compliance and fluid homeostasis.¹³ Animal models suggest that vessel pulsatility may modulate CSF flow, mixing with interstitial fluid, and facilitate brain interstitial fluid and metabolic waste clearance via meningeal lymphatics.¹⁴

We aimed to examine cranial arterial,⁶ venous,⁸ and CSF^{15–17} flow and pulsatility and clarify their cross-sectional and longitudinal associations with SVD burden and clinical outcomes. We examined how measures of

intracranial vessel stiffness were associated with SVD severity on imaging at baseline and 1-year clinical outcomes. We aimed to assess (1) how MRI-derived cerebrovascular stiffness associates with concurrent SVD features and (2) if altered baseline blood/CSF flow and pulsatility predict more severe 1-year SVD burden, cognitive decline, disability, or recurrent stroke or transient ischemic attack or incident infarcts on MRI.

METHODS

The prospective MSS3 (Mild Stroke Study 3; International Standard Randomised Control Trial Number [ISRCTN]:12113543) studies cross-sectional and longitudinal mechanisms, imaging, and clinical features of sporadic SVD.¹⁸ Full details of participant recruitment, assessments, and follow-up are published.^{18–20} Data underpinning this study and for the MSS3 in general are available upon written request to the corresponding author. In brief, we recruited patients with mild ischemic stroke (ie, nondisabling and modified Rankin Scale (mRS) score ≤ 2) of lacunar or nonlacunar (ie, minor cortical) ischemic stroke subtypes from National Health Service (NHS) Lothian, Scotland stroke services from 2018 to 2021 and followed them through 1 year (to 2022). Study recruitment and baseline assessment took place between August 2018 and October 2021, while completion of 1-year follow-up was in October 2022. The South East Scotland Research Ethics Committee (reference 18/SS/0044) approved the study, and all participants provided written informed consent. All patients received UK guideline stroke prevention therapies including antiplatelet, lipid-lowering, and antihypertensive drugs as appropriate. Those with poorly controlled heart rates were excluded from the study. Data acquisition and image analysis were blind to pulsatility/CBF measures, and all methods were validated.^{18,21–27} Per *Stroke* guidelines, we report against STROBE (Strengthening the Reporting of Observational Studies in Epidemiology).

We included the nonlacunar ischemic strokes as a comparator group for the lacunar strokes because both lacunar and nonlacunar strokes all receive the same secondary prevention drugs and have similar vascular risk factors of hypertension, smoking, hyperlipidemia, and diabetes, and we wished to control for the effect that these drugs or common risk factors might have on the pulsatility (and other vascular function) measures. All strokes were assessed for severity of SVD (WMH, lacunes, perivascular space [PVS], microbleeds, atrophy, and summary SVD score).

At baseline, we recorded hypertension, diabetes, hypercholesterolemia diagnosis, and smoking history. We assessed dependency (mRS)²⁸ and cognition (Montreal Cognitive Assessment)²⁹ at baseline and follow-up. We recorded any recurrent ischemic event (ie, new stroke/transient ischemic attack or MRI incident infarct) between baseline and follow-up.

We recorded supine blood pressure (BP) before baseline MRI and calculated pulse pressure as systolic BP minus diastolic BP. We did not gather data on BP variation in this cohort as it was beyond the scope of this study.

Magnetic Resonance Imaging

All participants underwent diagnostic imaging at the initial stroke presentation. At 1 to 3 months poststroke (to avoid acute effects)

and 1 year, we scanned participants using 3T MRI (MAGNETOM Prisma, Siemens Healthcare, Germany) with 3D T1w, T2w, fluid-attenuated inversion recovery, susceptibility-weighted imaging, and diffusion-weighted imaging (for full details, see Supplemental Methods and protocol article).¹⁸

At baseline only, we performed 3 separate 2D PC-MRI acquisitions to assess carotid arteries, venous sinuses, and CSF spaces (Figure 1A): one axial slice perpendicular to the external carotid arteries and ICAs at the spine C2-3 level (repetition time/echo time [TR/TE]=19.6/5.8 ms; flip angle, 12°; spatial resolution, 1.0×1.0 mm²; temporal resolution, 39.2 ms; and $v_{enc}=70$ cm/s), one coronal slice bisecting the superior sagittal sinus, straight sinus, and transverse sinuses (TR/TE=21.7/6.6 ms; flip angle, 12°; spatial resolution, 0.71×0.71 mm²; temporal resolution, 43.4 ms; and $v_{enc}=50$ cm/s), and one axial slice perpendicular to the C2-3 level spinal cord (TR/TE=25.2/8.5 ms;

flip angle, 12°; spatial resolution, 0.83×0.83 mm²; temporal resolution, 50.4 ms; and $v_{enc}=6$ cm/s). We interpolated the phase images across 32 timeframes, covering the cardiac cycle, using retrospective cardiac gating, a well-established multicenter study and trial method.^{8,30,31}

Image Analysis

Arterial, Venous, and CSF Flow Rates

We calculated the maximum PC-MRI signal magnitude across the cardiac cycle per pixel to help with vessel identification and drew regions of interest (ROIs) for the ICAs, vertebral arteries, internal jugular veins, superior sagittal sinus, straight sinus, and transverse sinuses lumens and subarachnoid CSF space at the foramen magnum using established methods.^{8,18} For each vessel, we calculated pixel velocities per timeframe using in-house

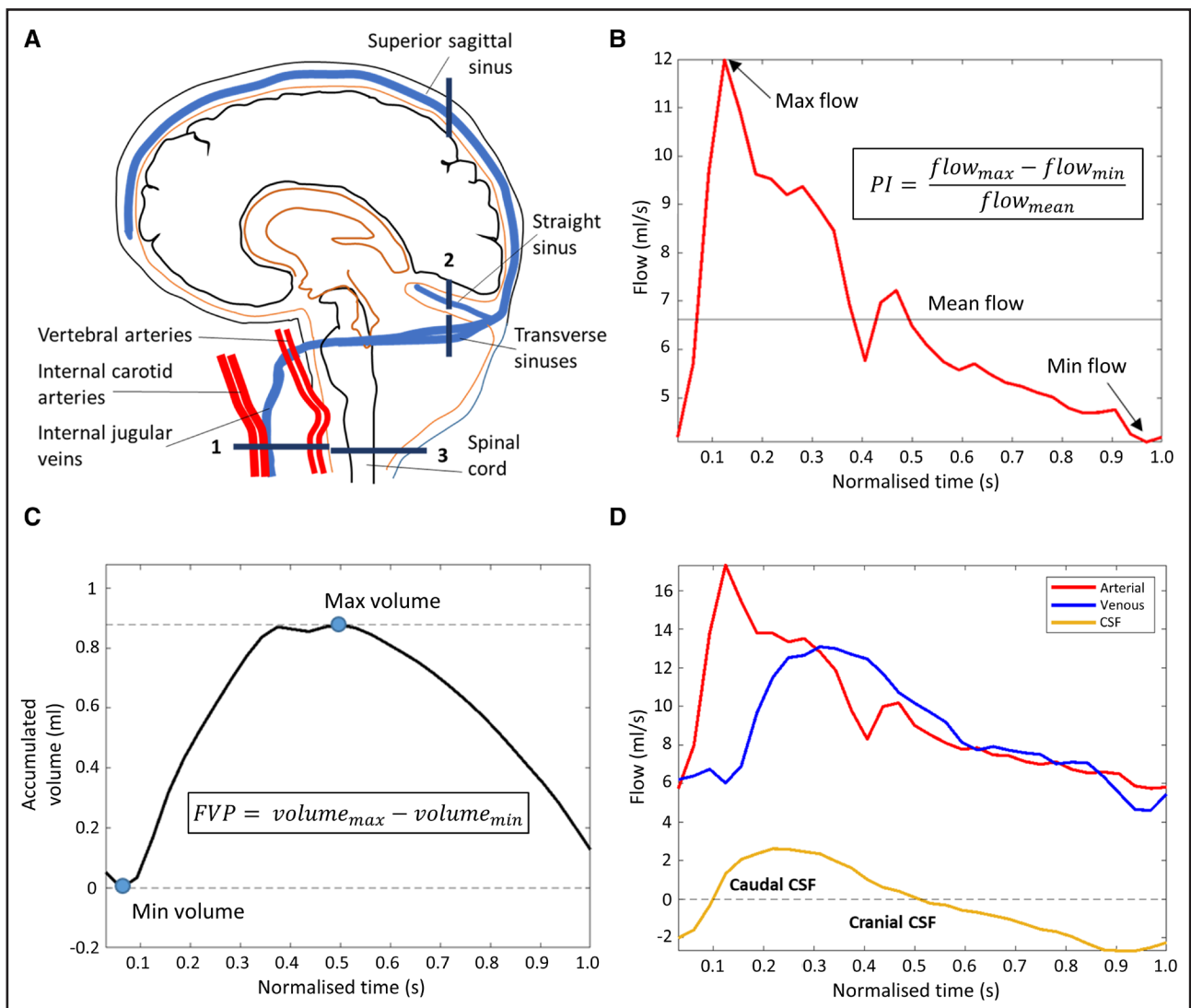


Figure 1. Measuring intracranial flow.

A, Phase-contrast magnetic resonance imaging slice locations: 1, an axial slice across the jugular veins, carotid, and vertebral arteries at C2-3 level of the spine; 2, a coronal slice across the venous sinuses; and 3, an axial slice across the spinal cord at C2-3 level. **B**, Internal carotid artery blood flow (mL/s) across the cardiac cycle. The horizontal line indicates the mean flow. **C**, The cumulative integrated flow volume across the cardiac cycle, after subtraction of the mean flow rate from the flow waveform and shifted to set minimum volume to zero. **D**, Absolute arterial, venous, and cerebrospinal fluid (CSF) flow across the cardiac cycle. Arterial inflow is followed by a rise in venous outflow, and more rapid efflux of CSF, to maintain pressure equilibrium. As blood drains via the veins, CSF flow reverses. FVP indicates flow volume pulsatility.

code (Matlab, version 9; MathWorks, Inc, United States), correcting for background error by subtracting the mean velocity calculated across an ROI placed over nearby stationary tissue.³² We multiplied velocities by pixel area and summed them to calculate the blood flow rate in mL/s to obtain a flow waveform across the cardiac cycle (Figure 1B).

We calculated CBF (mL/min) as the mean inflow (ICAs and vertebral arteries) per minute, normalized to brain volume¹⁸ to provide CBF/min per 100-mL brain volume.^{8,18} We calculated the pulsatility index (PI) and the resistance index (RI) using modified Gosling³³ and Pourcelot³⁴ equations ($PI = \frac{\text{flow}_{\max} - \text{flow}_{\min}}{\text{flow}_{\text{mean}}}$; $RI = \frac{\text{flow}_{\max} - \text{flow}_{\min}}{\text{flow}_{\max}}$; Figure 1B). We calculated combined arterial PI by summing flow waveforms across vertebral arteries and ICAs before using the equation. We calculated combined venous sinus PI as the mean of the PI values from each relevant vessel (summing waveforms was not appropriate due to them either being downstream of each other or originating from separate areas of the brain; Figure 1A). This was done for RI and flow volume pulsatility (FVP) also.

We calculated pulse transit time (PTT; a PWV indicator)⁸ by normalizing the cardiac cycle to 1 second and calculating the time difference between peak ICA and downstream vessel flow.^{8,35} For subarachnoid CSF PTT, only peak caudal flow was considered, as it corresponds to arterial inflow.³⁶ We excluded PTT measurements in cases where there was a difference in patient heart rate of >15 bpm between the relevant scans.

For blood flow volume analysis in all arteries and veins ROIs, we subtracted mean flow and plotted cumulative integration (Figure 1C). We calculated FVP (unitless) by subtracting minimum from maximum volume change across the cardiac cycle ($FVP = \frac{\text{volume}_{\max} - \text{volume}_{\min}}{\text{volume}_{\max}}$).⁵ We calculated net CSF flow by integrating the cranial (positive) and caudal (negative) flow values across the cardiac cycle, expressing net flow in mL/min,³⁰ and calculated peak CSF flow (mL/s) as the absolute maximum flow rate. We also calculated CSF stroke volume (mL), that is, average absolute flow volume.

Quantitative SVD Lesion Assessment

We used well-validated computational methods to measure baseline intracranial volume (ICV) and baseline and 1-year brain, WMH, and PVS volumes.^{21–23} In brief, using FSL-FLIRT, we coregistered all scans to the T2-w image. We determined ICV computationally by brain extraction from the susceptibility-weighted image. To determine WMH volume, we used an established pipeline^{18,22,23} to apply intensity-based thresholding to the fluid-attenuated inversion recovery scan and excluded false positives around the choroid plexus, aqueduct, third and fourth ventricles, using Freesurfer (<https://surfer.nmr.mgh.harvard.edu/>). In addition, to exclude hyperintensities unlikely to reflect pathology, we applied a lesion distribution probabilistic template to the thresholded images.²³ We manually excluded index and old infarcts and normalized WMH volume as %ICV. PVS volumes (mL) were segmented from the T2-w image using an established filter-based approach²³ in the basal ganglia (BG) and centrum semiovale (CSO) ROIs,^{21,23} and reported as % ROI volume. All masks were checked by experienced image analysts (S.W. and M.C.V.-H.) specialized in SVD and stroke and checked by J.M.W. Viewing was performed in high-quality neuroradiological standard viewing software reviewing the diffusion, fluid-attenuated inversion recovery, T2, and susceptibility-weighted imaging to ensure accuracy of

manual delineation of the acute and any old nonlacunar (cortical) or small subcortical infarcts. We visually rated structural images using the STRIVE-1 criteria (Standards for Reporting Vascular Changes on Neuroimaging 1).²⁵ We assessed periventricular and deep WMHs (Fazekas scale),²⁶ BG and CSO PVS score,²⁵ and the presence of microbleeds and lacunes to compute summary SVD score (0–4).²⁷ Scores were rated by 4 raters (X.L., J.Z., Y.C., and D.J.G.), and all readings were checked by an experienced neuroradiologist (J.M.W.).

Statistical Analysis

We performed all statistical analyses using R (version 3.6.1, Austria) in RStudio (version 1.2.5019, RStudio, Inc, United States). We assessed model diagnostics (histograms, QQ and heteroscedasticity plots, residual versus fitted values, and multicollinearity) to verify relevant assumptions. To give normally distributed residuals, we log10 transformed WMH (% ICV) and PVS (% ROI).

To assess factors associated with pulsatility, we used multivariable linear regression models, each with a flow/stiffness measure as the outcome and clinical features (ie, hypertension, diabetes, hypercholesterolemia diagnosis, and smoking history [ever/never] as predictors). To assess the relation of pulsatility measures to continuous imaging outcomes, we used flow/stiffness measures as predictor variables and SVD-related measures as outcome variables. All linear models are reported as regression coefficient of interest (B), 95% CI, and *P* value.

For binary (eg, recurrent stroke/transient ischemic attack) and ordinal (eg, SVD score) outcomes, we used logistic regression models and reported odds ratios (ORs) and 95% CIs. While *P* values are reported for ordinal logistic models, note that their interpretation can be challenging.³⁷ We grouped mRS categories with sparse data (scores, 2–5) to ensure there were sufficient data per category and satisfy the proportional odds assumption. As only 2 patients had died (ie, mRS score, 6) and composite outcomes including death may be problematic,³⁸ we excluded them from mRS analyses.

To assess longitudinal relationships, we used the follow-up variable of interest as the outcome, with the baseline value as an additional covariate.

Models were adjusted for age, sex, systolic BP, and baseline WMH volume/ICV %, consistent with previous work.³⁰ For baseline cross-sectional pulsatility analysis, we used all available arterial and venous stiffness measures (PI, RI, PTT, and FVP) in separate regression models but only PI in longitudinal pulsatility analyses, following a similar study.¹¹

We did not correct for multiple comparisons in this exploratory study but instead cautiously interpreted significance levels.

RESULTS

Population

We recruited 210 patients, of whom 205 (66.8% male; mean age, 66.4±11.1 years; Table 1) had usable baseline PC-MRI flow data (Figure 2). Ten of 205 patients had partial flow data and 198 full baseline SVD imagings. By 1 year, 2 patients had died, 186 of 203 attended follow-up assessment (mean, 380±37 days after

Table 1. Patient Summary Statistics

Baseline demographic and imaging variables (overall N=205)			
Demographic and health condition			
Age, y; median (range)	68.07 (32.74–86.34)		
Sex, male; N (%)	137 (66.83)		
Hypertension, N (%)	141 (68.78)		
Diabetes, N (%)	43 (20.98)		
Hypercholesterolemia, N (%)	150 (73.17)		
BP, mm Hg; mean±SD			
Systolic	149±20		
Diastolic	85±12		
MABP, mm Hg	106±13		
PP, mm Hg	64±19		
Heart rate, bpm*	64±11		
Time between index stroke and baseline assessment, d	61.09±20.64		
Time between baseline and follow-up assessment, d	380.09±37.12		
Smoking history, N (%)			
Never smoked	94 (45.85)		
Ever smoked	111 (54.15)		
Cerebral blood flow, mean±SD			
Total arterial flow, mL/min	582.95±108.52		
Total arterial flow, mL/min per 100-mL brain volume	53.83±9.54		
Pulsatility indices in brain vessels	PI	RI	FVP
Internal carotid artery	1.15±0.38	0.64±0.11	1.04±0.42
Vertebral artery	1.26±0.38	0.68±0.11	0.47±0.25
Superior sagittal sinus	0.52±0.22	0.40±0.12	0.34±0.18
Straight sinus	0.46±0.18	0.36±0.11	0.08±0.04
Transverse sinus	0.52±0.21	0.40±0.12	0.51±0.26
Internal jugular vein	1.01±0.49	0.64±0.21	0.97±0.64
CSF flow and pulsatility measures			
Net cervical CSF flow, mL/min†	2.23±5.32		
Cervical CSF stroke volume, mL	0.55±0.30		
Peak absolute cervical CSF flow, mL/s	2.46±1.33		
Pulse transit times (relative to arterial peak), s‡			
Superior sagittal sinus	0.15±0.10		
Straight sinus	0.12±0.12		
Transverse sinus	0.14±0.11		
Internal jugular vein	0.15±0.13		
Cervical CSF	0.06±0.09		
Baseline and 1-y follow-up features	Baseline	1-y follow-up	
Quantitative brain and SVD-related measures			
Brain volume, mL	1084.78±125.38	1075.66±123.43	
ICV, mL	1610.30±153.86	Not measured	
WMH volume, mL	8.20 (0.64–118.13)	8.31 (0.79–129.23)	
Brain volume/ICV, %	67.34 (51.16–78.70)	66.27 (52.77–78.97)	
WMH/ICV, %	0.51 (0.04–6.37)	0.51 (0.04–6.74)	
BG PVS volume, mL	2.74 (0.50–8.78)	2.46 (0.68–10.82)	
BG PVS/ROI volume, %	4.86 (0.67–12.26)	4.89 (1.58–18.43)	
CSO PVS volume, mL	11.08 (0.75–52.48)	9.10 (0.71–51.49)	

(Continued)

Table 1. Continued

Baseline demographic and imaging variables (overall N=205)		
CSO PVS/ROI volume, %	3.39 (0.22–13.86)	3.87 (0.25–19.09)
Total SVD score		
0	45 (21.95)	36 (20)
1	38 (18.54)	41 (22.78)
2	54 (26.34)	51 (28.33)
3	40 (19.51)	31 (17.22)
4	28 (13.66)	21 (11.67)
Cognition and disability		
MoCA score (maximum 30)	24.89±3.52	25.74±3.59
mRS score	1.02±0.68	1.96±0.96

BG indicates basal ganglia; BP, blood pressure; CSF, cerebrospinal fluid; CSO, centrum semiovale; FVP, flow volume pulsatility; ICV, intracranial volume; MABP, mean arterial blood pressure; MoCA, Montreal Cognitive Assessment; mRS, modified Rankin Scale; PI, pulsatility index; PP, pulse pressure; PVS, perivascular spaces; RI, resistance index; ROI, region of interest; SVD, small vessel disease; and WMH, white matter hyperintensity.

*Calculated in 2 steps: mean heart rate across all phase-contrast scans per patient and then mean heart rate across all patients.

†For the CSF flow, a positive value indicates flow in the cranial direction, while a negative value indicates flow in the caudal direction.

‡Based on standardized 1-second cardiac cycles.

baseline; 4 declined scans), and 17 were assessed via telephone/health records. For each analysis, we used all available data.

Due to heart rate differences of >15 bpm between pairs of PC-MRI acquisitions, we excluded 7 patients

from arterial-venous sinus PTT analysis and 7 patients from arterial-CSF PTT analysis.

We report baseline demographics, PC-MRI, baseline and 1-year quantitative brain volumes, SVD burden, and cognitive and disability measures summary statistics in

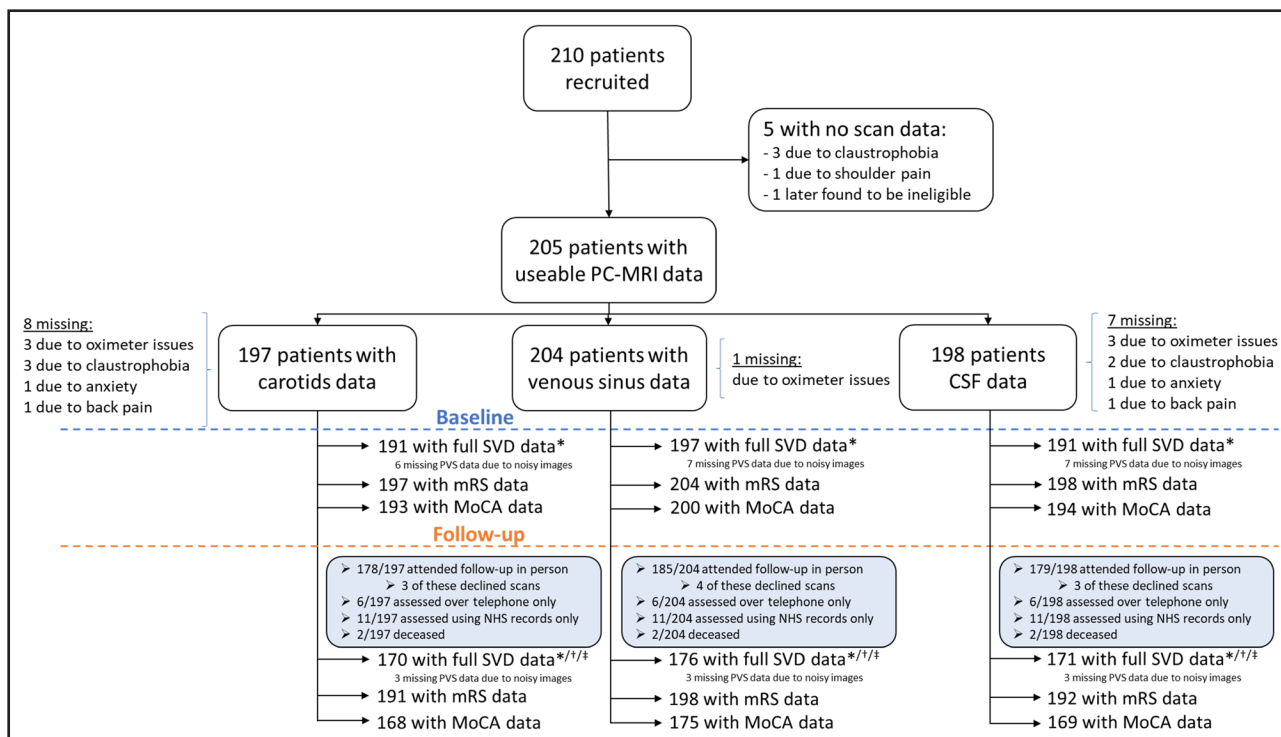


Figure 2. Patient flowchart for useable data.

Of the 210 patients recruited, 205 had partially complete flow data due to the reasons listed. We have shown the numbers of patients with data at baseline and follow-up visits. *Computational quantitative measurements, including brain volume. †One patient missing perivascular space (PVS) measurements due to a lack of a T2w scan. ‡One patient missed the microbleed assessment, and, therefore, SVD score, due to lack of susceptibility weighted imaging (SWI) scan. CSF indicates cerebrospinal fluid; MoCA, Montreal Cognitive Assessment; MRI, magnetic resonance imaging; mRS, modified Rankin Scale; NHS, National Health Service; PC, phase contrast; and SVD, small vessel disease.

Table 1. Although not used in the analyses here, Fazekas and PVS scores are shown in Table S1.

Baseline Cross-Sectional Associations

In separate models, we found that patients with higher arterial PI tended to have more WMH ($B=+0.260$ [95% CI, 0.077–0.442]), BG PVS ($B=+0.116$ [95% CI, 0.038–0.195]), and CSO PVS volume ($B=+0.094$ [95% CI, –0.017 to 0.206]; Table 2). Patients with higher arterial PI tended to be older and have higher pulse pressure, hypertension, and diabetes (Tables 3 and 4).

Mean venous sinus PI differed little with WMH, BG PVS, or CSO PVS volumes (eg, WMH: $B=+0.138$ [95% CI, –0.216 to 0.491]). Patients with higher mean venous sinus PI tended to be older, have higher pulse pressure, and be current/ex-smokers.

Patients with longer PTTs between the arteries and cervical CSF exhibited larger CSO PVS volumes ($B=+0.559$ [95% CI, 0.073–1.045]; Table 2), while current/ex-smokers had shorter PTTs in the venous sinuses.

Where we found associations with PI, we generally found similar associations with RI (eg, WMH \approx arterial RI: $B=+0.929$ [95% CI, 0.347–1.511]; Table 2), while higher FVPs associated with larger WMH volume (eg, WMH \approx arterial FVP: $B=+0.332$ [95% CI, 0.104–0.559]) associations with PVS volumes were uncertain (eg, BG PVS \approx arterial FVP: $B=+0.070$ [95% CI, –0.030 to 0.171]).

We found limited evidence of associations between CBF and any structural SVD-related measure (eg, WMH \approx CBF: $B=+0.003$ [95% CI, –0.004 to 0.009]; Table 2), but current/ex-smokers had higher CBF (Table 3).

We found little association between CSF flow or pulsatility measures and structural SVD features (Table 2).

Longitudinal Outcomes

We did not find definite associations between 1-year SVD burden and baseline arterial PI, venous sinus PI, total CBF, or CSF measures (Table 5; Figure 3), for example, 1-year WMH \approx arterial pulsatility: $B=+0.008$ (95% CI, –0.048 to 0.064). However, we found weak associations between higher 1-year BG PVS volume and both lower CBF ($B=-0.002$ [95% CI, –0.004 to 0.000]) and higher net foramen magnum CSF flow ($B=+0.002$ [95% CI, –0.001 to 0.006]). Patients with higher 1-year WMH volume tended to have higher CSF peak flow ($B=+0.012$ [95% CI, –0.001 to 0.025]).

We found limited associations between baseline vascular flow/pulsatility measures and 1-year clinical outcomes (eg, 1-year mRS \approx arterial PI: OR, 1.068 [95% CI, 0.472–2.643]), cognition (eg, 1-year Montreal Cognitive Assessment \approx arterial PI: $B=-0.106$ [95% CI, –1.443 to 1.230]), or recurrent ischemic events (eg, recurrent

event \approx arterial PI: OR, 1.196 [95% CI, 0.454–3.168]; Table 5). However, patients who had a recurrent ischemic event had lower baseline venous sinus PI (OR, 0.125 [95% CI, 0.015–0.897]), lower CSF stroke volume (OR, 0.300 [95% CI, 0.110–0.794]), and lower peak CSF flow associated with worse 1-year mRS (OR, 0.757 [95% CI, 0.605–0.941]).

DISCUSSION

We investigated potential cross-sectional and longitudinal relationships between intracranial arterial, venous, and CSF flow and pulsatility measures, baseline and 1-year SVD features, and clinical outcomes. We found that patients with higher arterial stiffness had larger baseline WMH and PVS volumes but only limited associations between pulsatility measures and 1-year imaging or clinical outcomes.

Intracranial Vascular Stiffness Measures

Cross-Sectional

Patients with larger WMH and PVS volumes had higher arterial pulsatility across several stiffness measures (PI, RI, and, for WMH volume, FVP), reflecting recent cross-sectional SVD studies.^{5,8} PIs of cerebral arteries have previously been shown to have a positive association with carotid-femoral PWV in healthy older adults,³⁹ which itself is positively associated with cross-sectional and longitudinal SVD severities.⁴⁰ Arterial pulsatility and WMH/PVS burden associations may partially reflect a coassociation with age but remain after age adjustment.⁴¹ Previously, higher arterial FVP, but not PI, was reported to be strongly associated with higher WMH volume.⁵ However, 4D PC-MRI sacrifices spatiotemporal resolution for acquisition volume⁴² versus 2D PC-MRI; hence, a greater partial volume effect in 4D PC-MRI may change the waveform, potentially explaining the disparity.⁴³

Unlike previous findings,^{8,30} we saw little association between venous sinus PI and SVD features. Hypotheses put forward include systolic arterial expansion producing pressure waves within the CSF spaces that are transmitted to the venous sinuses and increased capillary pulsatility (due to deficient dampening in the arteries) transmitted to the veins through blood flow. Increased venous sinus pulsatility may result from poor dampening upstream of the capillaries.

Intracranial PTT showed little relation to WMH volume, reflecting previous findings.⁸ We saw longer arterial-CSF PTTs in patients with larger CSO PVS volumes, suggesting a possible link between altered pulse propagation through the brain and enlarged PVS. Intracranial PTTs encompass several vascular beds and possess lower temporal resolution than PWV, which may measure propagation more accurately.⁴⁴ When assessing

Table 2. Regression Coefficients From Multivariable Baseline Analysis: Features of Cerebral Small Vessel Disease

Predictor variable (in separate models*)	Outcome variable								
	Log ₁₀ WMH vol/ICV†			Log ₁₀ basal ganglia PVS vol/ROI			Log ₁₀ centrum semiovale PVS vol/ROI		
	B	95% CI	P value	B	95% CI	P value	B	95% CI	P value
Arterial CBF, mL/min per 100-mL brain volume	0.003	−0.004 to 0.009	0.383	0.000	−0.003 to 0.003	0.84	0.001	−0.003 to 0.005	0.77
Pulsatility indices in brain vessels									
Arterial PI	0.260	0.077 to 0.442	0.006	0.116	0.038 to 0.195	0.004	0.094	−0.017 to 0.206	0.096
Arterial RI	0.929	0.347 to 1.511	0.002	0.400	0.153 to 0.647	0.002	0.272	−0.089 to 0.633	0.14
Arterial FVP	0.332	0.104 to 0.559	0.004	0.070	−0.030 to 0.171	0.17	0.030	−0.111 to 0.171	0.68
Venous sinus PI	0.138	−0.216 to 0.491	0.44	−0.011	−0.166 to 0.143	0.88	−0.147	−0.363 to 0.070	0.18
Venous sinus RI	0.258	−0.344 to 0.861	0.40	−0.006	−0.268 to 0.256	0.96	−0.188	−0.556 to 0.180	0.32
Venous sinus FVP	0.091	−0.332 to 0.514	0.67	−0.059	−0.242 to 0.125	0.53	−0.200	−0.456 to 0.057	0.13
IJV PI	0.057	−0.066 to 0.180	0.36	0.031	−0.021 to 0.082	0.25	0.020	−0.053 to 0.093	0.59
IJV RI	0.222	−0.072 to 0.515	0.14	0.073	−0.052 to 0.198	0.25	0.040	−0.135 to 0.215	0.65
IJV FVP	0.040	−0.055 to 0.135	0.40	0.012	−0.028 to 0.053	0.54	0.011	−0.045 to 0.067	0.69
CSF flow and pulsatility measures									
Net cervical CSF flow, mL/min	−0.003	−0.015 to 0.008	0.58	0.002	−0.003 to 0.007	0.54	0.000	−0.007 to 0.007	0.89
Cervical CSF stroke volume, mL	0.108	−0.102 to 0.317	0.31	0.030	−0.059 to 0.120	0.51	0.031	−0.095 to 0.156	0.63
Peak cervical CSF flow, mL/s	0.035	−0.011 to 0.082	0.13	0.008	−0.012 to 0.028	0.42	0.008	−0.020 to 0.036	0.57
PTT, s									
SSS	−0.224	−0.825 to 0.378	0.46	−0.044	−0.299 to 0.212	0.74	−0.192	−0.552 to 0.167	0.29
StS	−0.127	−0.661 to 0.407	0.64	0.002	−0.224 to 0.227	0.99	0.113	−0.205 to 0.430	0.49
TS	−0.251	−0.809 to 0.306	0.38	−0.124	−0.359 to 0.112	0.30	−0.225	−0.586 to 0.076	0.13
IJV	0.015	−0.450 to 0.480	0.95	0.020	−0.178 to 0.217	0.84	0.090	−0.186 to 0.366	0.52
Cervical CSF	0.612	−0.203 to 1.426	0.14	0.253	−0.100 to 0.606	0.16	0.559	0.073 to 1.045	0.024

CBF indicates cerebral blood flow; CSF, cerebrospinal fluid; FVP, flow volume pulsatility; ICV, intracranial volume; IJV, internal jugular vein; PI, pulsatility index; PTT, pulse transit time; PVS, perivascular space; RI, resistance index; ROI, region of interest; SSS, superior sagittal sinus; StS, straight sinus; TS, transverse sinus; and WMH, white matter hyperintensity.

*All models adjusted for age, sex, systolic blood pressure, and WMH/ICV %.

†Adjusted for age, sex, and blood pressure only. *P* values were reported to 2 significant figures up to 3 decimal places.

PTT, simultaneous measurement of vessels is preferable (as this allows for a true, synchronized snapshot of waveform propagation, avoiding errors introduced by temporal changes), but, due to flow velocity differences that affect the selection of velocity encoding, this was not technically viable using available PC-MRI methods. Our exclusion from PTT analysis of patients with notable heart rate disparities between sequences and normalizing cardiac cycles to 1 second should mitigate this limitation.

Stronger associations between arterial pulsatility and BG versus CSO PVS volume are consistent with previous findings,^{8,45} perhaps as BG PVS more strongly relates to higher BP/pulse pressure⁴⁵ or due to their proximity to larger blood vessels.

Longitudinal

Neither baseline arterial nor venous pulsatility is associated with 1-year SVD score, WMH, or PVS volume, despite clear SVD burden changes, including WMH volume increases and decreases. Previous studies that

found higher PWV with WMH progression^{46,47} measured PWV in large systemic not intracranial arteries as measured here.

Intracranial vessel pulsatility showed no clear associations with 1-year cognitive function or dependency. Greater 1-year decreases in cognitive function after acute stroke/transient ischemic attack were previously associated with increased middle cerebral artery but not ICA pulsatility (4D PC-MRI; N=89).⁵ We did, surprisingly, find that patients with lower baseline venous sinus and CSF pulsatility had higher 1-year odds of a recurrent ischemic event. Lower venous and CSF pulsatility could relate to impaired brain waste clearance, which could be associated with a worse disease burden and, therefore, a greater risk of stroke. The role of venous and CSF pulsatility in brain health requires further investigation.

While several cross-sectional studies⁶ found clear associations between higher pulsatility and worse SVD, mirroring our cross-sectional results, large longitudinal studies are scarce. Our findings are consistent with a

Table 3. Regression Coefficients From Multivariable Baseline Analysis: Age, Pulse Pressure, and Smoking History

Outcome variable (in separate models*)	Predictor variable								
	Age, y†			Pulse pressure			Smoking history‡		
	B	95% CI	P value	B	95% CI	P value	B	95% CI	P value
Pulse pressure	0.437	0.297 to 0.576	<0.001	NA			3.377	0.626 to 6.129	0.016
Arterial CBF, mL/min per 100-mL brain volume	0.064	−0.068 to 0.196	0.34	0.012	−0.119 to 0.143	0.86	3.527	0.934 to 6.119	0.008
Pulsatility indices in brain vessels									
Arterial PI	0.009	0.005 to 0.014	<0.001	0.011	0.007 to 0.015	<0.001	0.050	−0.041 to 0.140	0.28
Arterial RI	0.002	0.001 to 0.004	0.001	0.003	0.001 to 0.004	<0.001	0.022	−0.006 to 0.051	0.12
Arterial FVP	0.005	0.001 to 0.008	0.013	0.006	0.002 to 0.009	0.001	0.104	0.032 to 0.175	0.005
Venous sinus PI	0.007	0.004 to 0.009	<0.001	0.007	0.005 to 0.009	<0.001	0.052	0.005 to 0.098	0.029
Venous sinus RI	0.004	0.003 to 0.005	<0.001	0.004	0.003 to 0.005	<0.001	0.032	0.005 to 0.059	0.022
Venous sinus FVP	0.003	0.001 to 0.005	0.001	0.005	0.003 to 0.006	<0.001	0.036	−0.003 to 0.075	0.071
IJV PI	0.003	−0.003 to 0.010	0.33	0.007	0.000 to 0.014	0.036	0.224	0.089 to 0.360	0.001
IJV RI	0.001	−0.002 to 0.004	0.43	0.002	0.000 to 0.005	0.098	0.097	0.041 to 0.153	0.001
IJV FVP	−0.001	−0.010 to 0.008	0.75	0.006	−0.003 to 0.015	0.17	0.246	0.070 to 0.422	0.006
CSF flow and pulsatility measures									
Net cervical CSF flow, mL/min	0.027	−0.049 to 0.102	0.49	0.025	−0.050 to 0.010	0.51	0.581	−0.927 to 2.088	0.45
Cervical CSF stroke volume, mL	−0.004	−0.008 to 0.000	0.049	0.006	0.002 to 0.010	0.004	0.000	−0.082 to 0.082	0.99
Peak cervical CSF flow, mL/s	−0.019	−0.037 to 0.000	0.047	0.029	0.011 to 0.047	0.002	0.033	−0.337 to 0.403	0.86
PTT, s									
SSS	0.000	−0.002 to 0.001	0.67	−0.001	−0.002 to 0.001	0.37	−0.036	−0.065 to −0.008	0.014
StS	−0.001	−0.002 to 0.001	0.37	−0.001	−0.002 to 0.001	0.49	−0.036	−0.068 to −0.003	0.031
TS	0.000	−0.002 to 0.002	0.96	0.000	−0.002 to 0.001	0.63	−0.031	−0.062 to 0.001	0.06
IJV	0.000	−0.001 to 0.002	0.64	0.000	−0.001 to 0.002	0.71	0.006	−0.031 to 0.043	0.77
Foramen magnum CSF	0.000	−0.001 to 0.001	0.61	−0.001	−0.002 to 0.000	0.040	−0.012	−0.034 to 0.009	0.27

BP indicates blood pressure; CBF, cerebral blood flow; CSF, cerebrospinal fluid; FVP, flow volume pulsatility; ICV, intracranial volume; IJV, internal jugular vein; PI, pulsatility index; PTT, pulse transit time; RI, resistance index; SSS, superior sagittal sinus; StS, straight sinus; TS, transverse sinus; and WMH, white matter hyperintensity.

*All models adjusted for age, sex, systolic blood pressure, and WMH/ICV %.

†Adjusted for sex, systolic BP, and WMH/ICV % only.

‡Binary variable: never smoked vs ever smoked; B represents change with smoking. *P* values were reported to 2 significant figures up to 3 decimal places.

recent smaller study in N=122 healthy older subjects, suggesting that higher pulsatility does not predict 5-year WMH and PVS growth.¹¹ Indeed, a converse relationship was found although we cannot substantiate this due to lacking longitudinal pulsatility measurements.

Cerebral Blood Flow

We found sparse evidence of associations between CBF and SVD features though lower baseline CBF is weakly associated with larger 1-year PVS volume. While associations between CBF and longitudinal PVS volume change have not been explored previously to our knowledge, previous large-scale systematic reviews^{48,49} reported small studies showing cross-sectional associations between CBF and WMHs that attenuated in larger studies.⁴⁹ The few longitudinal studies mostly found that high WMH volumes predicted low CBF longitudinally,^{9,49} suggesting that low CBF is a consequence, not a cause, of SVD-related damage, generally consistent with our findings.

Estimating global CBF from the combined internal carotid and vertebral arterial inputs has limitations because it cannot account for contributions from other, small arteries. However, it is a reasonable proxy measure of global CBF that enables comparisons across the cohort when applied in a consistent manner, as done here. Other methods to measure CBF also have limitations; for example, for ASL, labeling efficiency can vary in patients with vascular changes, and many methods exclude the posterior fossa, thereby underestimating total CBF. Several studies have previously assessed regional CBF associations with vascular pathology,⁴⁹ with results indicating no clear cross-sectional relationship between WMH volume and CBF in normal-appearing white matter or gray matter, while lower CBF in the periventricular WMH penumbra was associated with WMH growth in healthy older participants. Therefore, it was not our intention here to measure regional CBF, which would be difficult to relate to arterial or venous pulsatility measures but to provide a global measure of CBF as a background setting for the pulsatility measures. In addition,

Table 4. Regression Coefficients From Multivariable Baseline Analysis: Hypertension, Diabetes, and Hypercholesterolemia

Outcome variable (in separate models*)	Predictor variable								
	Hypertension			Diabetes			Hypercholesterolemia		
	B	95% CI	P value	B	95% CI	P value	B	95% CI	P value
Arterial CBF, mL/min per 100-mL brain volume	−0.811	−3.810 to 2.189	0.60	0.618	−2.741 to 3.976	0.72	0.141	−2.814 to 3.096	0.93
Pulsatility indices in brain vessels									
Arterial PI	0.145	0.044 to 0.247	0.005	0.152	0.038 to 0.266	0.009	0.056	−0.046 to 0.158	0.28
Arterial RI	0.039	0.007 to 0.070	0.018	0.042	0.006 to 0.077	0.022	0.017	−0.014 to 0.049	0.29
Arterial FVP	0.051	−0.032 to 0.133	0.23	0.106	0.014 to 0.198	0.024	0.015	−0.067 to 0.097	0.72
Venous sinus PI	0.018	−0.035 to 0.071	0.51	0.011	−0.048 to 0.070	0.72	0.028	−0.024 to 0.081	0.29
Venous sinus RI	0.010	−0.021 to 0.041	0.53	0.009	−0.026 to 0.043	0.63	0.018	−0.013 to 0.049	0.25
Venous sinus FVP	0.022	−0.022 to 0.066	0.33	0.011	−0.038 to 0.061	0.66	0.015	−0.029 to 0.059	0.51
IJV PI	0.017	−0.141 to 0.175	0.83	0.029	−0.148 to 0.206	0.75	0.011	−0.145 to 0.167	0.89
IJV RI	0.012	−0.054 to 0.078	0.72	0.000	−0.074 to 0.073	0.99	0.001	−0.064 to 0.065	0.99
IJV FVP	0.079	−0.125 to 0.283	0.45	0.212	−0.015 to 0.438	0.067	−0.016	−0.217 to 0.186	0.88
CSF flow and pulsatility measures									
Net cervical CSF flow	−0.004	−1.722 to 1.714	1.00	−0.692	−2.603 to 1.219	0.48	−1.469	−3.149 to 0.210	0.086
Cervical CSF stroke volume	−0.069	−0.162 to 0.024	0.15	0.013	−0.091 to 0.117	0.80	0.019	−0.073 to 0.111	0.69
Peak cervical CSF flow	−0.135	−0.555 to 0.285	0.53	0.211	−0.257 to 0.678	0.38	0.146	−0.269 to 0.560	0.49
PTT, s									
SSS	−0.009	−0.043 to 0.024	0.58	−0.009	−0.047 to 0.028	0.62	−0.024	−0.057 to 0.008	0.15
StS	0.005	−0.033 to 0.042	0.80	−0.047	−0.089 to −0.006	0.026	−0.028	−0.064 to 0.009	0.14
TS	−0.020	−0.056 to 0.015	0.27	−0.023	−0.063 to 0.017	0.26	−0.025	−0.060 to 0.011	0.17
IJV	0.016	−0.026 to 0.058	0.45	−0.013	−0.060 to 0.034	0.60	−0.018	−0.059 to 0.024	0.40
CSF	−0.010	−0.039 to 0.019	0.51	0.014	−0.013 to 0.042	0.30	0.002	−0.023 to 0.026	0.90

CBF indicates cerebral blood flow; CSF, cerebrospinal fluid; FVP, flow volume pulsatility; IJV, internal jugular vein; PI, pulsatility index; PTT, pulse transit time; RI, resistance index; SSS, superior sagittal sinus; StS, straight sinus; and TS, transverse sinus.

*All models adjusted for age, sex, systolic blood pressure, and white matter hyperintensity/intracranial volume %. *P* values were reported to 2 significant figures up to 3 decimal places.

normalizing each participant's CBF measurement to their brain volume accounted for differences in brain size and atrophy, enabling more accurate comparisons.

CSF Measures

We found some associations between worse mRS, lower CSF stroke volume, and peak flow (potentially due to a link between impaired brain waste clearance affecting cognition), but CSF flow and pulsatility generally showed little association with SVD features (except as below). Enlarged PVSs suggest sluggish interstitial fluid movement, but exact mechanisms remain unclear. The lack of associations is consistent with some previous findings^{8,17} but not others.^{15,16} One previous study¹⁶ used amplitude transfer functions to describe CSF pulse waves, which could explain the difference. We previously found that CSF stroke volume and PVS score were weakly associated but did not assess PVS volume.³⁰

We found a 2.23-mL/s net foramen magnum CSF flow rate cranially, perhaps due to measurement errors,

pathology, or net CSF movement to drainage pathways primarily exiting from the skull (cribriform plate, meningeal, perivascular, and perineural).⁵⁰ Interestingly, we found a small trend between higher peak CSF flow and larger 1-year WMH volume, while lower CSF stroke volume and peak flow were associated with higher 1-year mRS score, suggesting that CSF dynamics may be associated with SVD-related dependency. Animal models exhibit a relationship between CSF, brain interstitial fluid flow, and waste clearance,¹⁴ but the exact relationship in humans and possible links with SVD remain undetermined.

Strengths and Weaknesses

Strengths of this study include the large (>200) sample, highly phenotyped clinically, for baseline and 1-year SVD features using well-established methods, assessing PVS and WMH, contemporaneous arterial, venous and CSF flow analyses, multiple vessel stiffness/pulsatility measures, clinical outcomes, and a relevant control group that accounts for medication. Currently, this is the largest such longitudinal study. We did not include a healthy

Table 5. Adjusted Regression Analyses for SVD-Related Volumes at 1 Year

Predictor variable at baseline (in separate models*)	Outcome variable at 1-y follow-up											
	Log ₁₀ WMH vol/ICV			Log ₁₀ basal ganglia PVS vol/ROI			Log ₁₀ centrum semiovale PVS vol/ROI			Brain tissue volume, mL		
	B	95% CI	P value	B	95% CI	P value	B	95% CI	P value	B	95% CI	P value
Arterial CBF	0.001	−0.001 to 0.003	0.38	−0.002	−0.004 to 0.000	0.082	−0.001	−0.004 to 0.001	0.27	0.201	−0.134 to 0.535	0.24
Pulsatility indices in brain vessels												
Arterial PI	0.008	−0.048 to 0.064	0.78	0.015	−0.044 to 0.074	0.62	−0.004	−0.082 to 0.073	0.91	1.774	−8.270 to 11.818	0.73
Venous sinus PI	−0.083	−0.190 to 0.024	0.13	−0.012	−0.127 to 0.104	0.84	−0.016	−0.169 to 0.137	0.83	10.559	−10.964 to 32.082	0.33
CSF flow and pulsatility measures												
Net cervical CSF flow	0.001	−0.002 to 0.004	0.63	0.002	−0.001 to 0.006	0.14	0.002	−0.002 to 0.006	0.39	−0.556	−1.167 to 0.054	0.074
Cervical CSF stroke volume	0.041	−0.018 to 0.099	0.17	−0.035	−0.097 to 0.028	0.27	−0.016	−0.100 to 0.067	0.71	−8.983	−2.812 to 20.777	0.14
Peak cervical CSF flow	0.012	−0.001 to 0.025	0.081	−0.004	−0.018 to 0.010	0.56	0.000	−0.019 to 0.018	0.96	1.894	−0.729 to 4.518	0.16
Predictor variable at baseline (in separate models*)	Outcome variable at 1-y follow-up											
	Summary SVD score			mRS score			MoCA score			Recurrent ischemic event (Y/N)		
	OR	95% CI	P value	OR	95% CI	P value	B	95% CI	P value	OR	95% CI	P value
Arterial CBF	1.012	0.973 to 1.052	0.54	0.991	0.961 to 1.022	0.57	−0.029	−0.074 to 0.015	0.19	1.003	0.969 to 1.038	0.86
Pulsatility indices in brain vessels												
Arterial PI	1.044	0.317 to 3.448	0.94	1.068	0.427 to 2.643	0.89	−0.106	−1.443 to 1.230	0.88	1.196	0.454 to 3.168	0.72
Venous sinus PI	0.240	0.024 to 2.306	0.22	1.971	0.347 to 11.259	0.44	−0.034	−2.679 to 2.610	0.80	0.125	0.015 to 0.897	0.045
CSF flow and pulsatility measures												
Net cervical CSF flow	1.008	0.940 to 1.080	0.82	0.977	0.930 to 1.025	0.34	0.019	−0.056 to 0.094	0.62	0.967	0.910 to 1.026	0.27
Cervical CSF stroke volume	1.666	0.473 to 5.915	0.43	0.300	0.110 to 0.794	0.017	0.080	−1.399 to 1.559	0.92	0.104	0.399 to 3.627	0.74
Peak cervical CSF flow	1.045	0.791 to 1.382	0.75	0.757	0.605 to 0.941	0.013	0.039	−0.287 to 0.364	0.81	1.078	0.846 to 1.374	0.54

CBF indicates cerebral blood flow; CSF, cerebrospinal fluid; ICV, intracranial volume; MoCA: Montreal Cognitive Assessment; mRS, modified Rankin Scale; OR, odds ratio; PI, pulsatility index; PVS, perivascular space; ROI, region of interest; SVD, small vessel disease; and WMH, white matter hyperintensity.

*All models adjusted for age, sex, baseline systolic blood pressure, baseline WMH/ICV %, and baseline measurement of the outcome variable. WMH and PVS volumes were reported as % of ICV and ROIs, respectively.

control group because it would not account for medication effects, or comorbidities, and would add little²; instead, we recruited patients with nonlacunar strokes as controls for lacunar (SVD) stroke and a broad range of disease burdens. Weaknesses include the lack of follow-up PC-MRI and the limited PC-MRI spatial and temporal resolutions, meaning that only a limited number of vessels could be assessed, in particular smaller, penetrating vessels were not examined. Longer follow-up duration may be needed to detect some SVD-related outcomes and should include regional CBF measures. In the future, we may explore the relationship between pulsatility and BP variation and analyze structural images over longer follow-up periods.

Conclusions

Despite clear cross-sectional associations between pulsatility and SVD, neither baseline intracranial arterial, venous, or CSF pulsatility nor CBF had major effects on 1-year clinical or imaging outcomes. As a recent smaller study with longer follow-up suggested, pulsatility and stiffness may result from, rather than cause, SVD damage. Imaging in early SVD stages may be needed to identify predictive pulsatility measures. Further research should assess the order of these changes, whether pulsatility differs between patients with SVD progression versus regression, and how we may intervene in SVD progression.

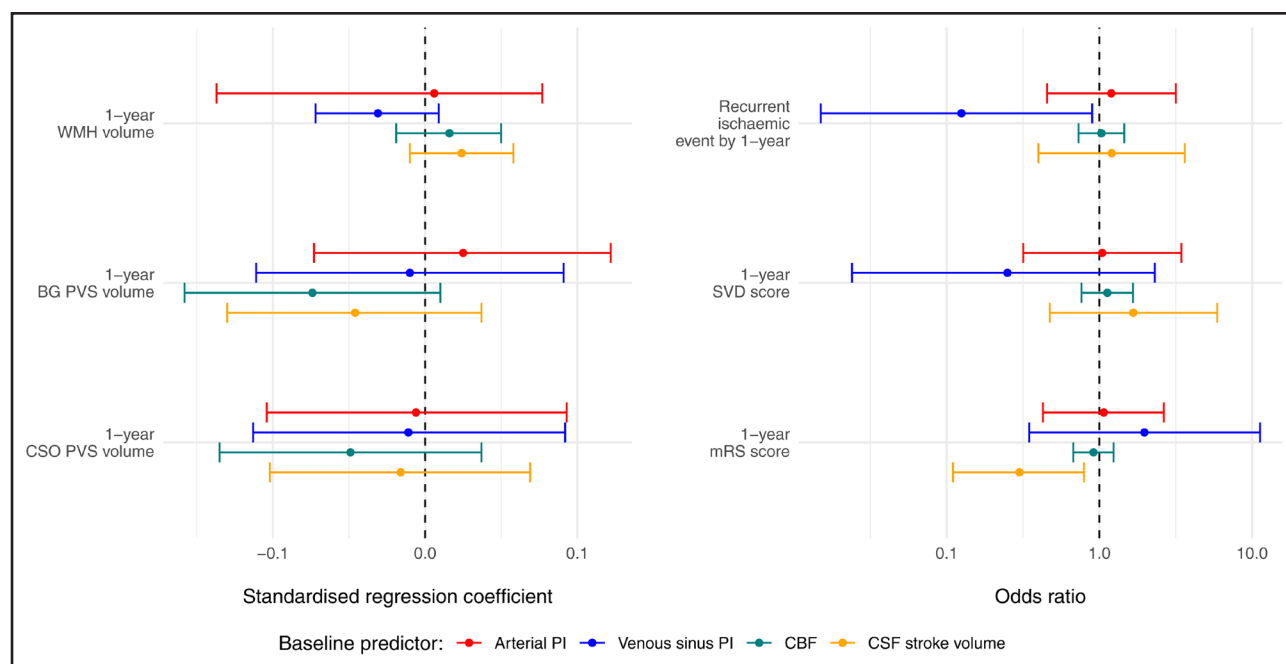


Figure 3. Forest plot summarizing longitudinal flow/pulsatility index (PI) and small vessel disease (SVD) feature analyses.

A, Standardized regression coefficients between SVD features and arterial PI, mean venous sinus PI, cerebral blood flow (CBF), and cerebrospinal fluid (CSF) stroke volume. The dots represent the standardized coefficients, and the solid lines represent 95% CIs. **B**, Odds ratios on a log₁₀ scale between intracranial flow and pulsatility measures and SVD, dependency, and recurrent ischemic event ordinal and binary outcomes. Dots show odds ratios, and solid lines show 95% CIs. Note that for visualization, we scaled the odds ratio of CBF in tens of mL/min per 100-mL brain volume. BG indicates basal ganglia; CSO, centrum semiovale; mRS, modified Rankin Scale; PVS, perivascular space; and WMH, white matter hyperintensity.

ARTICLE INFORMATION

Received August 30, 2024; final revision received April 1, 2025; accepted May 23, 2025.

Affiliations

Department of Neuroimaging Sciences, Centre for Clinical Brain Sciences, The University of Edinburgh, United Kingdom (A.G.M., M.J.T., M.S.S., F.M.C., M.C.V.-H., S.W., R.B., E. Sakka, D.J.G., E. Sleight, C.M., R.D.C., D.J., A.J., C.A.R., U.C., I.M., F.N.D., J.M.W.). UK Dementia Research Institute at The University of Edinburgh, Edinburgh Medical School, United Kingdom (A.G.M., M.J.T., M.S.S., F.M.C., M.C.V.-H., S.W., R.B., E. Sakka, D.J.G., E. Sleight, C.M., R.D.C., D.J., A.J., C.A.R., U.C., I.M., F.N.D., J.M.W.). University of Foreigners of Perugia, Italy (L.B.). Department of Neurology, West China Hospital of Sichuan University, Chengdu (Y.C.). Division of Neurology, Department of Medicine, The University of Hong Kong, China (X.L.). Department of Neurology, Shanghai General Hospital, Shanghai Jiao Tong University School of Medicine, China (J.Z.).

Acknowledgments

The authors thank Agnieszka Czechon, Rachel Locherty, and the Edinburgh Imaging radiographers.

Sources of Funding

This work was supported by Medical Research Scotland Studentship (to Dr Morgan; grant PhD-1165-2017) partnered with Siemens Healthineers; Siemens; UK Dementia Research Institute that receives its funding from DRI Ltd, primarily funded by the UK Medical Research Council and Alzheimer's Society; Fondation Leducq Network for the Study of Perivascular Spaces in Small Vessel Disease (16 CVD 05); Stroke Association Post-Doctoral Fellowships (to Drs Stringer and Wiseman; grants SAPDF 23/100007 and 18/100026), Small Vessel Disease-Spotlight on Symptoms (grant SAPG 19\1000680), and Garfield Weston Foundation Senior Clinical Lectureship (to Dr Doubal; grant TSALECT 2015/04); The Mrs Gladys Row Fogo Charitable Trust Center for Research into Aging and the Brain; NHS Research Scotland (to Dr Doubal); the British Heart Foundation Edinburgh center for Research Excellence (grant RE/18/5/34216); the NHS Lothian Research and Development Office (to Dr Thrippleton); the European Union

Horizon 2020, PHC-03-15, project No666881, SVDs@Target (to Dr Stringer); the Chief Scientist Office of Scotland Clinical Academic Fellowship (to Dr Clancy; grant CAF/18/08); the Stroke Association Princess Margaret Research Development Fellowship (to Dr Clancy; grant 2018), and CONACYT (Consejo Nacional de Ciencia y Tecnología; National Council of Science and Technology), the Rowling Clinic and Row Fogo Charitable Trust as above (to Dr Arteaga Reyes); Medical Research Council (National Productivity Fund MR/R502327/1; to Dr Sleight); Wellcome Trust Translational Neuroscience Ph.D. Programme (grant 224912/Z/21/Z; to Dr Jamie Garcia); the Alzheimer's Society (ref 486 [grant AS-CP-18b-001]); the University of Edinburgh College of Medicine and Veterinary Medicine (to Dr Jochems); and the Scottish Funding Council through the Scottish Imaging Network: A Platform for Scientific Excellence Collaboration. The 3T scanner is funded by the Wellcome Trust (grant 104916/Z/14/Z), the Dunhill Trust (grant R380R/1114), the Edinburgh and Lothians Health Foundation (grant 2012/17), the Muir Maxwell Research Fund, and The University of Edinburgh.

Disclosures

Siemens Healthineers provided partial PhD studentship support (to Dr Morgan) but had no role in the study. Prof Wardlaw reports academic grants that funded the research as listed in the Sources of Funding, which had no role in the study design, conduct, analysis, or interpretation, including the Wellcome Trust, the Medical Research Council, the Stroke Association, the Biotechnology and Biological Sciences Research Council, the Weston Brain Institute, the Alzheimer's Society, Fondation Leducq, the Horizon 2020 Framework Programme, Chief Scientist Office, the Dunhill Medical Trust, the Mrs Gladys Row Fogo Charitable Trust, and the British Heart Foundation. The other authors report no conflicts.

Supplemental Material

Supplemental Methods
Table S1

REFERENCES

- Sutton-Tyrrell K, Najjar SS, Boudreau RM, Venkitchalam L, Kupelian V, Simonsick EM, Havlik R, Lakatta EG, Spurgeon H, Kritchevsky S, et al; Health

- ABC Study. Elevated aortic pulse wave velocity, a marker of arterial stiffness, predicts cardiovascular events in well-functioning older adults. *Circulation*. 2005;111:3384–3390. doi: 10.1161/CIRCULATIONAHA.104.483628
2. Wardlaw JM, Smith C, Dichgans M. Small vessel disease: mechanisms and clinical implications. *Lancet Neurol*. 2019;18:684–696. doi: 10.1016/S1474-4422(19)30079-1
 3. Kohn JC, Lampi MC, Reinhart-King CA. Age-related vascular stiffening: causes and consequences. *Front Genet*. 2015;6:112. doi: 10.3389/fgene.2015.00112
 4. Sagawa K, Lie RK, Schaefer J. Translation of Otto Frank's paper "Die Grundform des Arteriellen Pulses" Zeitschrift für Biologie 37: 483–526 (1899). *J Mol Cell Cardiol*. 1990;22:253–254. doi: 10.1016/0022-2828(90)91459-k
 5. Birnefeld J, Wahlin A, Eklund A, Malm J. Cerebral arterial pulsatility is associated with features of small vessel disease in patients with acute stroke and TIA: a 4D flow MRI study. *J Neurol*. 2020;267:721–730. doi: 10.1007/s00415-019-09620-6
 6. Shi Y, Thrippleton MJ, Marshall I, Wardlaw JM. Intracranial pulsatility in patients with cerebral small vessel disease: a systematic review. *Clin Sci (Lond)*. 2018;132:157–171. doi: 10.1042/CS20171280
 7. Geurts LJ, Zwanenburg JUM, Klijn CJM, Luijten PR, Biessels GJ. Higher pulsatility in cerebral perforating arteries in patients with small vessel disease related stroke, a 7T MRI study. *Stroke*. 2019;50:62–68. doi: 10.1161/STROKEAHA.118.022516
 8. Shi Y, Thrippleton MJ, Blair GW, Dickie DA, Marshall I, Hamilton I, Doubal FN, Chappell F, Wardlaw JM. Small vessel disease is associated with altered cerebrovascular pulsatility but not resting cerebral blood flow. *J Cereb Blood Flow Metab*. 2018;40:85–99. doi: 10.1177/0271678x18803956
 9. van der Veen PH, Muller M, Vincken KL, Hendrikse J, Mali WP, van der Graaf Y, Geerlings MI; SMART Study Group. Longitudinal relationship between cerebral small-vessel disease and cerebral blood flow: the second manifestations of arterial disease-magnetic resonance study. *Stroke*. 2015;46:1233–1238. doi: 10.1161/STROKEAHA.114.008030
 10. Kneihl M, Hofer E, Enzinger C, Niederkorn K, Horner S, Pinter D, Fandler S, Eppinger S, Haidegger M, Schmidt R, et al. Intracranial pulsatility in relation to severity and progression of cerebral white matter hyperintensities. *Stroke*. 2020;51:3302–3309. doi: 10.1161/STROKEAHA.120.030478
 11. Vikner T, Karalija N, Eklund A, Malm J, Lundquist A, Gallewicz N, Dahlin M, Lindenberger U, Riklund K, Bäckman L, et al. 5-Year associations among cerebral arterial pulsatility, perivascular space dilation, and white matter lesions. *Ann Neurol*. 2022;92:871–881. doi: 10.1002/ana.26475
 12. Singer J, Trollor JN, Baune BT, Sachdev PS, Smith E. Arterial stiffness, the brain and cognition: a systematic review. *Ageing Res Rev*. 2014;15:16–27. doi: 10.1016/j.arr.2014.02.002
 13. Mokri B. The Monro-Kellie hypothesis: applications in CSF volume depletion. *Neurology*. 2001;56:1746–1748. doi: 10.1212/wnl.56.12.1746
 14. Wardlaw JM, Benveniste H, Nedergaard M, Zlokovic BV, Mestre H, Lee H, Doubal FN, Brown R, Ramirez J, MacIntosh BJ, et al; colleagues from the Fondation Leducq Transatlantic Network of Excellence on the Role of the Perivascular Space in Cerebral Small Vessel Disease. Perivascular spaces in the brain: anatomy, physiology and pathology. *Nat Rev Neurol*. 2020;16:137–153. doi: 10.1038/s41582-020-0312-z
 15. Beggs CB, Magnano C, Shepherd SJ, Belov P, Ramasamy DP, Hagemeyer J, Zivadinov R. Dirty-appearing white matter in the brain is associated with altered cerebrospinal fluid pulsatility and hypertension in individuals without neurologic disease. *J Neuroimaging*. 2016;26:136–143. doi: 10.1111/jon.12249
 16. Henry-Feugeas MC, Roy C, Baron G, Schouman-Claeys E. Leukoaraiosis and pulse-wave encephalopathy: observations with phase-contrast MRI in mild cognitive impairment. *J Neuroradiol*. 2009;36:212–218. doi: 10.1016/j.neurad.2009.01.003
 17. Jolly TA, Bateman GA, Levi CR, Parsons MW, Michie PT, Karayanidis F. Early detection of microstructural white matter changes associated with arterial pulsatility. *Front Hum Neurosci*. 2013;7:782. doi: 10.3389/fnhum.2013.00782
 18. Clancy U, Garcia DJ, Stringer MS, Thrippleton MJ, Valdes-Hernandez MC, Wiseman S, Hamilton I, Chappell FM, Brown R, Blair GW, et al. Rationale and design of a longitudinal study of cerebral small vessel diseases, clinical and imaging outcomes in patients presenting with mild ischaemic stroke: mild stroke study 3. *Eur Stroke J*. 2021;6:81–88. doi: 10.1177/2396987320929617
 19. Sleight E, Stringer MS, Clancy U, Arteaga-Reyes C, Jaime Garcia D, Jochems AC, Wiseman S, Valdes Hernandez M, Chappell FM, Doubal FN, et al. Association of cerebrovascular reactivity with 1-year imaging and clinical outcomes in small vessel disease: an observational cohort study. *Neurology*. 2024;103:e210008.
 20. Clancy U, Arteaga-Reyes C, Jaime Garcia D, Hewins W, Locherty R, Valdés Hernández MDC, Wiseman SJ, Stringer MS, Thrippleton MJ, Chappell FM, et al. Incident infarcts in patients with stroke and cerebral small vessel disease: frequency and relation to clinical outcomes. *Neurology*. 2024;103:e209750. doi: 10.1212/WNL.000000000000209750
 21. Ballerini L, Lovreglio R, Valdes Hernandez MDC, Ramirez J, MacIntosh BJ, Black SE, Wardlaw JM. Perivascular spaces segmentation in brain MRI using optimal 3D filtering. *Sci Rep*. 2018;8:2132. doi: 10.1038/s41598-018-19781-5
 22. Valdes Hernandez Mdel C, Armitage PA, Thrippleton MJ, Chappell F, Sandeman E, Munoz Maniega S, Shuler K, Wardlaw JM. Rationale, design and methodology of the image analysis protocol for studies of patients with cerebral small vessel disease and mild stroke. *Brain Behav*. 2015;5:e00415. doi: 10.1002/brb3.415
 23. Valdés Hernández LMD, Glatz A, Aribisala BS, Bastin ME, Dickie DA, Duarte Coello R, Munoz Maniega S, Wardlaw JM. Edinburgh DataShare: 2023. doi: 10.7488/ds/7486
 24. Ballerini L, Booth T, Valdes Hernandez MDC, Wiseman S, Lovreglio R, Munoz Maniega S, Morris Z, Pattie A, Corley J, Gow A, et al. Computational quantification of brain perivascular space morphologies: associations with vascular risk factors and white matter hyperintensities. A study in the Lothian Birth Cohort 1936. *Neuroimage Clin*. 2020;25:102120. doi: 10.1016/j.nicl.2019.102120
 25. Wardlaw JM, Smith EE, Biessels GJ, Cordonnier C, Fazekas F, Frayne R, Lindley RI, O'Brien JT, Barkhof F, Benavente OR, et al. Neuroimaging standards for research into small vessel disease and its contribution to ageing and neurodegeneration. *Lancet Neurol*. 2013;12:822–838. doi: 10.1016/S1474-4422(13)70124-8
 26. Fazekas F, Chawluk JB, Alavi A, Hurtig HI, Zimmerman RA. MR signal abnormalities at 1.5 T in Alzheimer's dementia and normal aging. *Am J Roentgenol*. 1987;149:351–356. doi: 10.2214/ajr.149.2.351
 27. Staals J, Makin SD, Doubal FN, Dennis MS, Wardlaw JM. Stroke subtype, vascular risk factors, and total MRI brain small-vessel disease burden. *Neurology*. 2014;83:1228–1234. doi: 10.1212/WNL.0000000000000837
 28. van Swieten JC, Koudstaal PJ, Visser MC, Schouten HJ, van Gijn J. Interobserver agreement for the assessment of handicap in stroke patients. *Stroke*. 1988;19:604–607. doi: 10.1161/01.str.19.5.604
 29. Nasreddine ZS, Phillips NA, Bédirian V, Charbonneau S, Whitehead V, Collin I, Cummings JL, Chertkow H. The Montreal Cognitive Assessment, MoCA: a brief screening tool for mild cognitive impairment. *J Am Geriatr Soc*. 2005;53:695–699. doi: 10.1111/j.1532-5415.2005.53221.x
 30. Blair GW, Thrippleton MJ, Shi Y, Hamilton I, Stringer M, Chappell F, Dickie DA, Andrews P, Marshall I, Doubal FN, et al. Intracranial hemodynamic relationships in patients with cerebral small vessel disease. *Neurology*. 2020;94:e2258–e2269. doi: 10.1212/WNL.0000000000009483
 31. Stringer MS, Blair GW, Kopczak A, Kerkhofs D, Thrippleton MJ, Chappell FM, Maniega SM, Brown R, Shuler K, Hamilton I, et al; The SVDs@target consortium. Cerebrovascular function in sporadic and genetic cerebral small vessel disease. *Ann Neurol*. 2024;97:483–498. doi: 10.1002/ana.27136
 32. Walker PG, Cranney GB, Scheidegger MB, Waseleski G, Pohost GM, Yoganathan AP. Semiautomated method for noise reduction and background phase error correction in MR phase velocity data. *J Magn Reson Imaging*. 1993;3:521–530. doi: 10.1002/jmri.1880030315
 33. Gosling RG, King DH. Arterial assessment by Doppler-shift ultrasound. *Proc R Soc Med*. 1974;67:447–449. doi: 10.1177/00359157740676P113
 34. Pourcelot L. Applications cliniques de l'examen Doppler transcutané. *Coloques de l'Inst Natl Santé Rech Med*. 1974;34:213–240. https://catalog.nlm.nih.gov/discovery/fulldisplay?docid=alma9911158713406676&context=L&vid=01NLM_INST:01NLM_INST&lang=en&search_scope=MyInstitution&adaptor=Local%20Search%20Engine&tab=LibraryCatalog&query=ids56,contains,Cerebrovascular%20Disorders%20--%20diagnosis,AND&mode=advanced&offset=140
 35. Stoquart-Elsankari S, Balédent O, Gondry-Jouet C, Makki M, Godefroy O, Meyer M-E. Aging effects on cerebral blood and cerebrospinal fluid flows. *J Cereb Blood Flow Metab*. 2007;27:1563–1572. doi: 10.1038/sj.jcbfm.9600462
 36. Greitz D, Wirestam R, Franck A, Nordell B, Thomsen C, Stahlberg F. Pulsatile brain movement and associated hydrodynamics studied by magnetic resonance phase imaging. The Monro-Kellie doctrine revisited. *Neuroradiology*. 1992;34:370–380. doi: 10.1007/BF00596493
 37. McShane BB, Gal D, Gelman A, Robert C, Tackett JL. Abandon statistical significance. *Am Stat*. 2019;73:235–245. doi: 10.1080/00031305.2018.1527253

38. Cordoba G, Schwartz L, Woloshin S, Bae H, Gotsche PC. Definition, reporting, and interpretation of composite outcomes in clinical trials: systematic review. *BMJ*. 2010;341:c3920. doi: 10.1136/bmj.c3920
39. Fico BG, Miller KB, Rivera-Rivera LA, Corkery AT, Pearson AG, Eisenmann NA, Howery AJ, Rowley HA, Johnson KM, Johnson SC, et al. The impact of aging on the association between aortic stiffness and cerebral pulsatility index. *Front Cardiovasc Med*. 2022;9:821151. doi: 10.3389/fcvm.2022.821151
40. Álvarez-Bueno C, Medrano M, Lucerón-Lucas-Torres M, Otero-Luis I, López-López S, Lever-Megina CG, Caverro-Redondo I. Association between pulse wave velocity and white matter hyperintensities among older adults: a meta-analysis of cross-sectional and longitudinal studies. *Ageing Res Rev*. 2024;101:102501. doi: 10.1016/j.arr.2024.102501
41. Aribisala BS, Morris Z, Eadie E, Thomas A, Gow A, Valdés Hernández MC, Royle NA, Bastin ME, Starr J, Deary IJ, et al. Blood pressure, internal carotid artery flow parameters, and age-related white matter hyperintensities. *Hypertension*. 2014;63:1011–1018. doi: 10.1161/HYPERTENSIONAHA.113.02735
42. Morgan AG, Thrippleton MJ, Wardlaw JM, Marshall I. 4D flow MRI for non-invasive measurement of blood flow in the brain: a systematic review. *J Cereb Blood Flow Metab*. 2021;41:206–218. doi: 10.1177/0271678X20952014
43. Morgan AG, Thrippleton MJ, Stringer M, Jin N, Wardlaw JM, Marshall I. Repeatability and comparison of 2D and 4D flow MRI measurement of intracranial blood flow and pulsatility in healthy individuals and patients with cerebral small vessel disease. *Front Psychol*. 2023;14:1125038. doi: 10.3389/fpsyg.2023.1125038
44. Fu X, Huang C, Wong KS, Chen X, Gao Q. A new method for cerebral arterial stiffness by measuring pulse wave velocity using transcranial Doppler. *J Atheroscler Thromb*. 2016;23:1004–1010. doi: 10.5551/jat.33555
45. Del Brutto OH, Mera RM; Atahualpa Project Investigators. Enlarged basal ganglia perivascular spaces are associated with pulsatile components of blood pressure. *Eur Neurol*. 2018;79:86–89. doi: 10.1159/000486308
46. Rosano C, Watson N, Chang Y, Newman AB, Aizenstein HJ, Du Y, Venkatraman V, Harris TB, Barinas-Mitchell E, Sutton-Tyrrell K. Aortic pulse wave velocity predicts focal white matter hyperintensities in a biracial cohort of older adults. *Hypertension*. 2013;61:160–165. doi: 10.1161/HYPERTENSIONAHA.112.198069
47. King KS, Chen KX, Hulsey KM, McColl RW, Weiner MF, Nakonezny PA, Peshock RM. White matter hyperintensities: use of aortic arch pulse wave velocity to predict volume independent of other cardiovascular risk factors. *Radiology*. 2013;267:709–717. doi: 10.1148/radiol.13121598
48. Shi Y, Thrippleton MJ, Makin SD, Marshall I, Geerlings MI, de Craen AJM, van Buchem MA, Wardlaw JM. Cerebral blood flow in small vessel disease: a systematic review and meta-analysis. *J Cereb Blood Flow Metab*. 2016;36:1653–1667. doi: 10.1177/0271678X16662891
49. Stewart CR, Stringer MS, Shi YL, Thrippleton MJ, Wardlaw JM. Associations between white matter hyperintensity burden, cerebral blood flow and transit time in small vessel disease: an updated meta-analysis. *Front Neurol*. 2021;12:647848. doi: 10.3389/fneur.2021.647848
50. Koh L, Zakharov A, Johnston M. Integration of the subarachnoid space and lymphatics: is it time to embrace a new concept of cerebrospinal fluid absorption? *Cerebrospinal Fluid Res*. 2005;2:6. doi: 10.1186/1743-8454-2-6